UDC 621. 314. 22. 027. 8

DEVELOPMENTS IN FUJI LARGE POWER TRANSFORMERS

By Sadao Maekawa
Yoshiaki Ikeda

Chiba Factory

I. INTRODUCTION

Paralleling the continuously increasing demand for electric power energy, there has been a remarkable expansion of extra-high voltage transmission systems and installation of larger thermal power stations. We have been confronted with the necessity of manufacturing transformers in larger sizes and in higher voltage classes within severe transport limits which, especially in Japan, narrow railway loading gauge imposes upon us. This has compelled transformer designers to develop new forms of construction which make the best use of materials and space within transformers.

Some representative transformers manufactured by Fuji Electric and their features are given below:

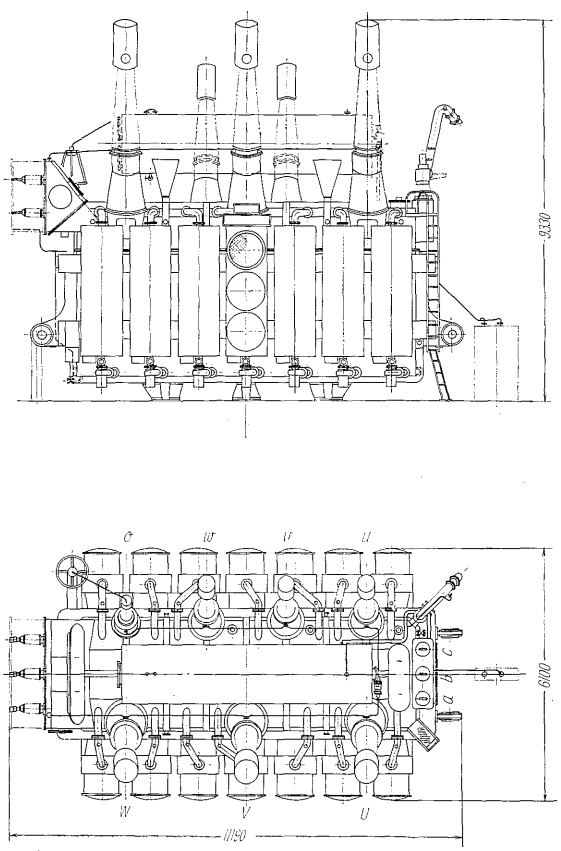

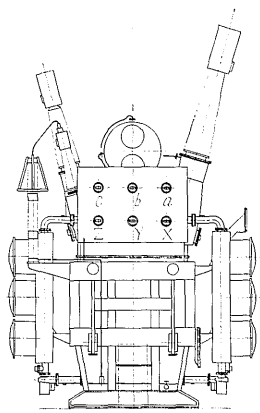

Fig. 2 Outline of 275 kv 345 Mva transformer

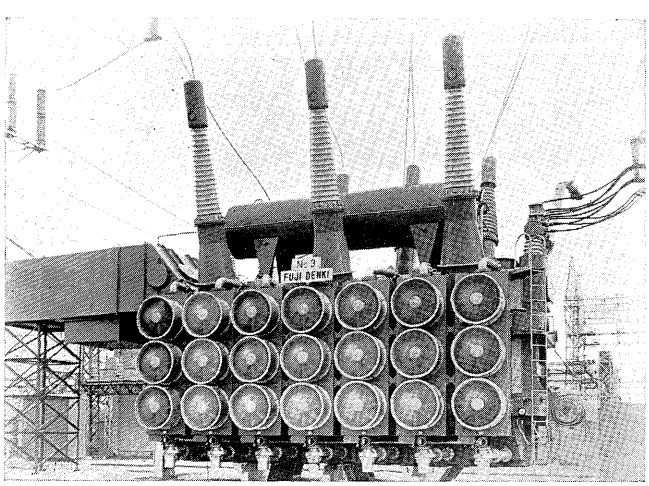

Fig. 1 View of 275 kv 345 Mva transformer

(1) 275 kv 345 Mva transformer for Nagoya Substation (Electric Power Development Co., Ltd.) (See *Fig. 1* and *Fig. 2*)

3ϕ 60 cps 300/300/90 Mva 275–262.5^{R}/154/11 kv
Star/star/delta BIL 1050/750/150 kv
Impedance: P–S 10.2%/S–T 9%/P–T 22.5%
Forced oil circulation: Fan cooled
Total weight: 345 tons
Transport weight: 240 tons

The main impedance between the h.v. and m.v. windings is much lower than the standard 14% in 275 kv systems, because this transformer was made for operation in parallel with an existing 90/90/45 Mva transformer. Generally the lower the impedance, the greater the weight. This is due to the fact that the ratio of core

to winding weight increases and the electromagnetic forces during fault conditions become greater and more severe. This largest unit was transported in the completely constructed state by rail using our " Schnabel " wagon.

(2) 275 kv 345 Mva on-load tap-changing transformer for Chita Substation (Chubu Electric Power Co., Inc.)

3ϕ 60 cps 300/300/90 Mva $275^{R}{}^{+8}_{-8} \times 3.125$/154/33 kv

Star/star/delta BIL 1050/750/200 kv

Impedance : P–S 14%/S–T 12.75%/P–T 30%

Forced oil circulation : Fan cooled

Total weight : 385 tons

Transport weight : 246 tons

Direct on-load tap-changing at the neutral of the 275 kv side.

A tertiary current limiting reactor is connected to restrict the short-circuit capacity of the tertiary system. This reactor is arranged in a corner of the transformer tank.

This transformer is transported by ship.

(3) 275/220 kv 200 Mva autotransformer for Himeji Substation (Kansai Electric Power Co., Inc.)

3ϕ 60 cps 200/200 Mva $275/220^{R}{}^{+14}_{-2} \times 2.5$ kv

Star/star

Impedance : 4.36%

This is the first on-load tap-changing autotransformer with indirect voltage regulation for interconnection between 275 kv and 220 kv transmission lines in our country. The connection of this autotransformer is given in *Fig. 3*.

(4) 500 kv autotransformer (model)

1ϕ 50 cps

$500/\sqrt{3}/275^{R}{}^{+8}_{-8} \times 3.4375/\sqrt{3}/15$ kv

BIL 1925/1050/150 kv

Ac test level 860/460/50 kv 1 minute

This autotransformer was planned for use in investigating the insulation and other peculiar technical problems, which are expected with the coming introduction of 500 kv transmission systems in Japan. The on-load tap-changing equipment is connected directly to the 275 kv line side. New types of oscillation-free cylindrical layer windings were developed for both series and parallel windings. The outer view of this autotransformer is illustrated in *Fig. 4*.

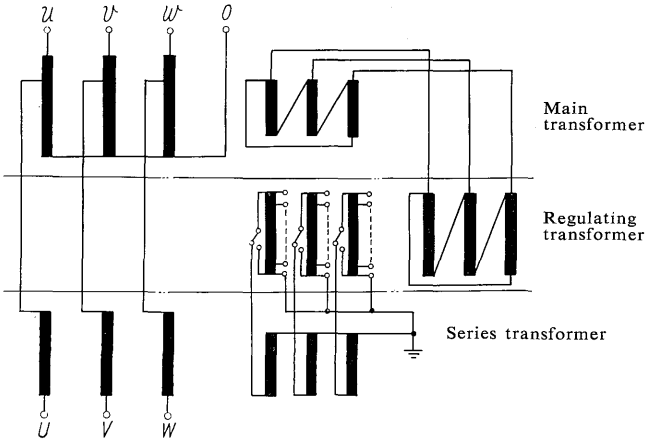

Fig. 3 Connection of 275/220 kv 200 Mva autotransformer

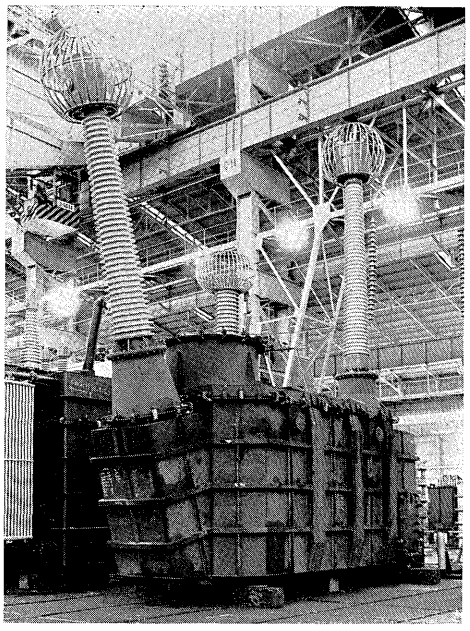

Fig. 4 View of $\frac{500}{\sqrt{3}}/\frac{275}{\sqrt{3}}$ kv autotransformer

The purpose of this paper is to illustrate our latest and original technology concerning some features of large power transformers.

II. CORES

According to our practice, large power transformers are of core type construction, using cold-rolled grain-oriented silicon steel sheet of the best loss class available. Since the introduction of grain-oriented steel sheets, much work has been done on the cutting and annealing processes to gain high core quality and reduce scrap. Mitred corners are adopted to make the flux run parallel to the direction of rolling for as much of the magnetic path length as possible. The angle of miter is fixed at 45° and overlap is achieved by varying the position of adjacent laminations.

The core is usually five-limbed for larger three phase units of more than 200 Mva. The yokes and the outer limbs have 60% of the cross sectional area of the main limbs, which results in about an 80% reduction in height as compared with the corresponding three-limbed core. This saving is most important on very large transformers. The 45° cut joint is also applied to five-limbed cores regardless of the difference in cross-sectional area of the main

limbs and yokes. This joint form has proved to give lower core loss than other joint forms which cut the sheets at an angle other than 45°.

The limbs are divided by cooling ducts which limit the maximum core temperature to a safe and acceptable value. The arrangement of the cooling ducts, which make parallel magnetic paths, or the ratio of the cross-sectional area of yokes or outer limbs to main limbs in five-limbed cores has much influence on flux distribution in the core. This flux distribution in each part of the core is calculated with the aid of a digital computer, considering the non-linear exciting characteristics of the core, and the core loss is estimated in respective parts of the core. The optimum choice of cross-sectional area thus obtained enables adoption of high flux density and smaller core weight.

III. WINDINGS

The cylindrical or disc type winding is applied in accordance with the voltage or current class. Selecting some typical windings of larger units, details are illustrated below.

1. Oscillation-free Cylindrical Layer Winding

For voltage classes 154 kv and above, especially with directly grounded neutrals, this winding has been used with marked success. Each concentrically arranged successive layer is shorter than the preceding one. Therefore the trapezoid-formed winding utilizes the core window effectively. The static shield is connected to the outer-most layer. Higher series capacitance between layers gives practically linear impulse voltage distribution and no internal voltage oscillation occurs. Two successive layers can be connected in two ways. *Fig. 5* (a) shows the N-connection using the layers all wound in the same direction, and *Fig. 5* (b) illustrates the U-connection using pairs of layers wound in different directions. The U-connection has the merit of easier inner connection between layers.

However, at the end of the layer, the voltage between adjacent layers becomes twice that of the corresponding N-connection.

For 500 kv autotransformers, we have developed an inner N-connection for series winding and a V-connection for parallel winding. The inner N-connection is shown in *Fig. 5* (c). The connecting lead is arranged in the narrow gap between two successive layers. Careful consideration has been taken in determining the dimension of the connecting lead and its insulation. To avoid corona erosion, corona measurement was performed on many test pieces, some results of which will be referred to later.

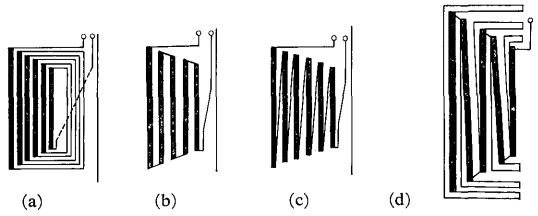

(a) N-connection (b) U-connection
(c) Inner N-connection (d) V-connection

Fig. 5 Oscillation-free cylindrical layer winding

The V-connection is shown in *Fig. 5* (d). In order to reduce the radial dimension of the conventional U-connection, the cross-section of the layer insulation paper is made triangular, and only one end of this layer insulation is extended and flanged outwards. Every other conductor layer is wound slightly inclined to the vertical. However, the gradient is so small that it does not influence the mechanical strength of the winding.

In accomplishing these developments, we were able to neglect the connecting lead which was formerly arranged in the outer space of the winding and to adopt solid insulation between the tank and winding, at the same time reducing its insulation distance and the overall size of the transformer.

Oscillation-free cylindrical layer winding has other well-known merits. As the neutral (which is directly grounded or reduced in insulation level) is in the layer next to the l.v. winding, much smaller insulation space to the l.v. winding is necessary. Surge transfer from the h.v. winding becomes much lower than the basic impulse level of the l.v. winding.

The axially balanced AT distribution causes no great axial forces or stresses under short-circuit.

2. Special Twin-Disc Winding

As the intermediate voltage winding for voltages of 110 kv or 154 kv and for larger current, the special twin-disc winding is preferred because a comparatively large number of parallel conductors demands easier connection of coil sections rather than the ideal impulse voltage characteristics achieved by the high series capacitance of complex interleaved connections.

As shown in *Fig. 6,* the winding is divided into two parallel circuits, the ends of which are respectively led to the outer and inner sides of electrostatic shield rings at the upper and lower ends of the winding and connected together there. Each circuit is of course composed of parallel copper strands transposed continuously. Common insulated conductor is generally used for this purpose.

Coil sections with odd numbers 1, 3, 5.....are connected in series similar to a conventional twin-disc winding, and interleave the coil sections with even numbers 2, 4, 6.....which are also connected in the same way.

As the insulation of the connecting lead between every other section against the interleaved coil section utilizes space which is obtained by not completing the electrical turns, it is not necessary to afford dimensional margin in the width of the winding.

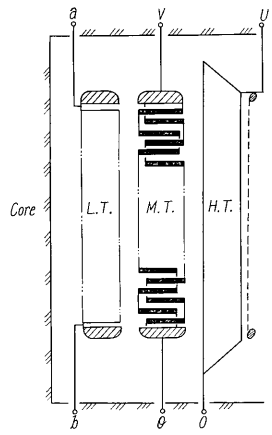

Fig. 6 Special twin-disc winding

If the total number of coil sections is $2N$, the voltage between adjacent coil sections v_n is given by

$$v_n = \frac{E}{N} \qquad E = \text{Applied voltage (ac)}$$

This value is 1/2 that of the conventional twin-disc winding. Hence the horizontal duct between coil sections can be reduced and a higher winding space factor obtained.

3. Multiple Shielded Winding

Multiple shielded winding is adopted to control the oscillatory behavior to which the combined sets of transformers are subject when excited by an impulse voltage. Two examples are illustrated in the following.

(1) *Fig. 7* illustrates the arrangement of windings of the series transformer, which is connected to the l.v. side of the autotransformer with indirect voltage regulation shown in *Fig. 7*. The end faces of the secondary winding of the series transformer (l.v. line side) are provided with electrostatic shield rings. Two sheets of shielding which surround the winding are respectively connected to its top and bottom ends, as shown by dotted lines in *Fig. 7*. The initial voltage distribution can be estimated by the capacitive equivalent circuit given in *Fig. 8*. Where

K_s, K_c, K: Total series capacitance of the series winding, parallel-winding of the main autotransformer and the secondary winding of the series transformer.

C: Total parallel capacitance of the secondary winding of the series transformer.

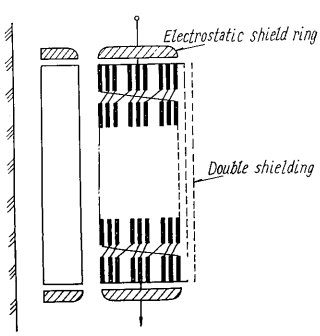

Fig. 7 Double static shielding in series transformer of autotransformer

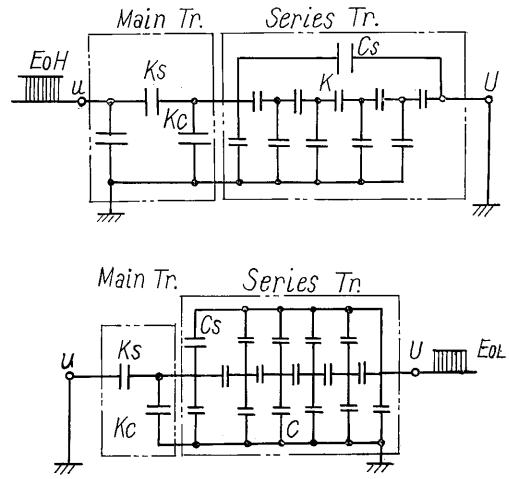

Fig. 8 Capacitive equivalent circuit of the autotransformer

C_s: Capacitance between the double electrostatic shields of the series transformer.

When terminal U is grounded and the impulse voltage is impressed on terminal u, or vice versa, the ground-charging current surges through capacitance C_s and the stress between turns or terminals of the series transformer is restricted to a reasonable value.

(2) Multiple shielded winding is also applied successfully to combined sets of large main transformers and direct on-load tap-changing series transformers on the neutral side of the main transformers.

As shown in *Fig. 7*, multiple sheets of electrostatic shielding are arranged concentrically around the tap winding of the series transformer. The impulse voltage e_x at connecting point x under the impact of impulse voltoge on the h.v. line terminal is given approximately by,

$$e_x = e_L \varepsilon^{-at} - (e_L - e_C)\cos \omega t$$

where

$$e_L = \frac{L_2}{L_1 + L_2} E$$

$$e_C = \frac{K_1}{K_1 + K_2 + C_2 + C_3} E$$

$$\omega = \sqrt{\frac{L_1 L_2}{L_1 + L_2 (K_1 + K_2 + C_2 + C_3)}}$$

L_1, L_2: Equivalent inductance of the h.v. winding of the main transformer, and of the tap winding of the series transformer.

C_2: Capacitance between the neutral side

layer of the h.v. and l.v. windings of the main transformer.

K_1 : Series capacitance of the h.v. winding of the main transformer.

C_3 : Parallel capacitance of the tap winding of the series transformer, which is mainly controlled by the multiple electrostatic shield.

K_2 : Series capacitance of the tap winding of the series transformer.

As understood from the above equation, impulse voltage at connecting point x can be controlled to a minimum by making e_L equal to e_C, i.e. making the second term zero.

Accordingly the additional capacitance of the multiple electrostatic shields is used for control the initial voltage distribution to equal quasistationary voltage distribution. Consequently any compensating voltage oscillation can not occur.

As the effect of this method has been found remarkably effective, protective devices such as arresters and condensers are not necessary at the connecting point.

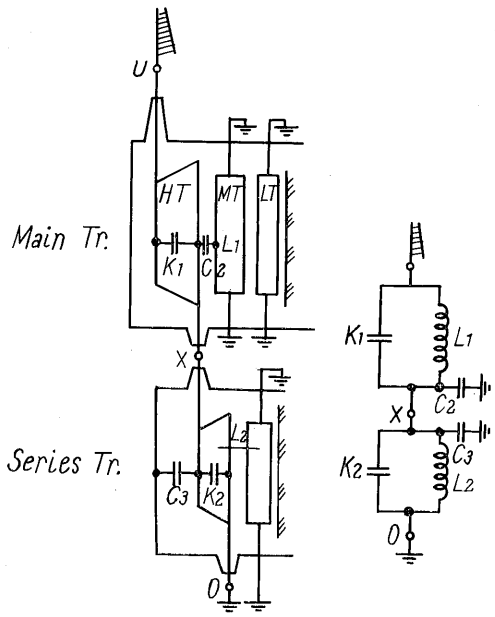

Fig. 9 Combined set of main transformer and direct on-load tap-changing series transformer

IV. STRAY LOAD LOSSES

The amount of leakage flux traversing the windings increases with transformer ratings, particularly in high impedance units. This relationship can be deduced, if we make the following simplifying assumptions :

(1) The leakage flux has an axial component only.

(2) The dimension of the active part of the transformer is propotional to $(\text{kva})^{0.25}$

The total leakage flux ϕ_l is estimated by

$$\phi_l = Bl \cdot \left(\frac{wh_1}{2} + \alpha + \frac{wh_2}{2}\right) \cdot L$$

where

Bl = Maximum leakage flux density

wh_1, wh_2 = Breadth of h.v. and l.v. windings

α = Insulation space between h.v. and l.v. windings

L = Mean length of h.v. and l.v. windings

H = Height of h.v. and l.v. windings

N = Number of turns

f = Frequency

ϕ_m = Main flux in the core

% impedance of transformer is given by

$$\%Z = \frac{ZI}{E} \cdot 100$$

$$Z \propto \frac{fN^2}{H}\left(\frac{wh_1}{3} + \alpha + \frac{wh_2}{3}\right)L$$

By rough approximation,

$$\left(\frac{wh_1}{2} + \alpha + \frac{wh_2}{2}\right) \propto \left(\frac{wh_1}{3} + \alpha + \frac{wh_2}{3}\right)$$

$$\%Z \propto \frac{\frac{fN^2}{H}\left(\frac{wh_1}{3} + \alpha + \frac{wh_2}{3}\right) \cdot LI}{fN\phi_m} \propto \frac{\phi_l}{\phi_m}$$

$$\therefore \quad \phi_l \propto \%Z \cdot \phi_m \propto \%Z \cdot (\text{kva})^{0.5}$$

Thus the total leakage flux ϕ_l is approximately proportional to the impedance and the main flux ϕ_m, or $(\text{kva})^{0.5}$.

Therefore eddy-current losses in the winding and stray load losses may attain considerable magnitude in large power transformers and their reduction is one of the most important problems in transformer design.

The leakage flux density in radial and axial components, and the eddy-current loss distribution in the winding can be calculated with a digital computer.

Fig. 10 is an example of calculated data

The program has proved capable of predicting the eddy current loss in the winding with satisfactory accuracy.

The ratio of eddy-current loss to I^2R loss in the winding is approximately estimated by

% eddy-current loss $\propto$

$$\left(\frac{f \cdot NQ \cdot b}{H}\right)^2 \propto (f(\text{kva})^{0.25} \cdot b)^2$$

where b = breadth of conductor vertical to the direction of leakage flux, Q = cross-section of conductors.

If the % eddy-current loss in the winding is to be kept constant, the size of the conductor should be chosen inversly propotional to $(\text{kva})^{0.25}$. Although this causes some complication, the windings of larger units are usually composed of multiple parallel conductors of the smallest size possible. These multiple conductors are transposed continuously or at suitable places of the winding to equalize the impedance of each path.

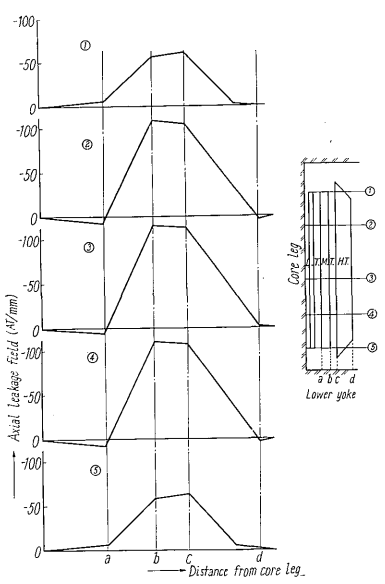

(a) Distribution of axial leakage field

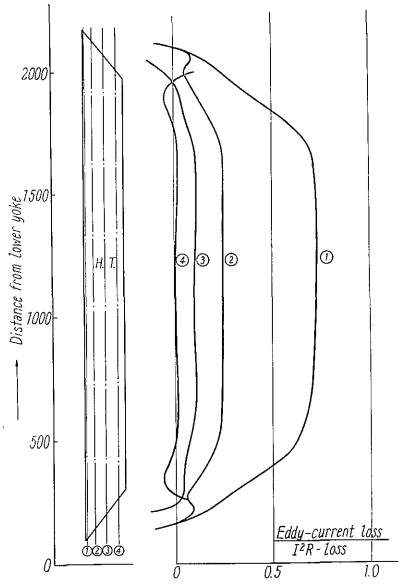

(c) Eddy-current loss distribution in the h. v. winding

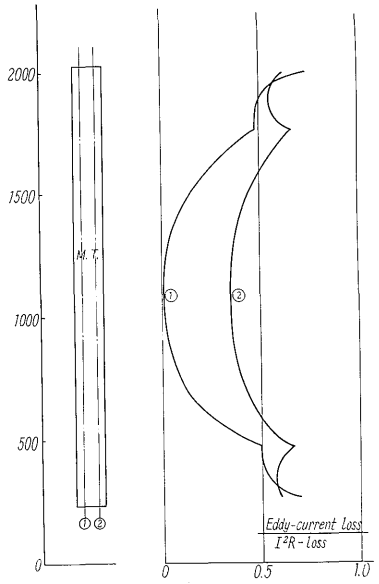

(d) Eddy-curent loss distribution in the m. v. winding

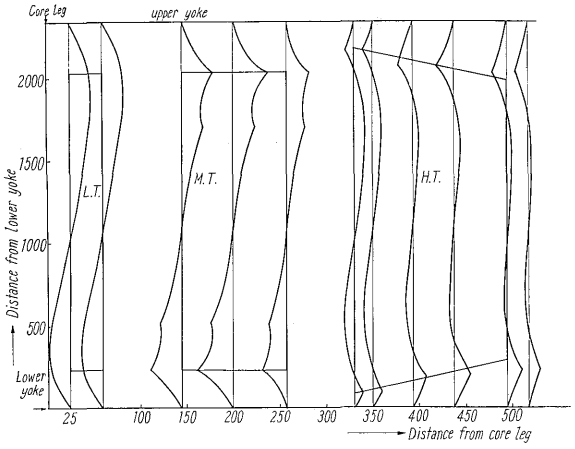

(b) Distribution of radial leakage field

Fig. 10 Distribution of leakage flux and eddy-current losses in the windings

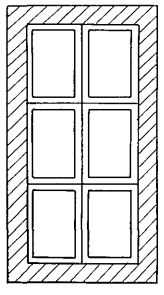

Fig. 11 Common insulated conductor

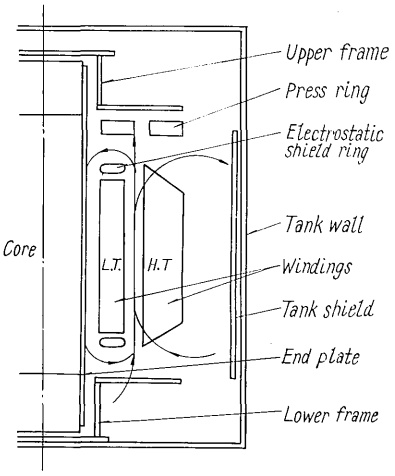

Fig. 12 Leakage flux and structures of transformer

The leakage flux is constrained mainly in an axial direction at the center of the winding. At the ends of the winding, however, the leakage flux spreads for return paths and so acquires a radial component. Hence the conductor size is reduced in breadth at the center and in height at the ends so that the cross-sectional area of the conductor may be constant.

Common insulated conductor has been increasingly used for the windings of large power transformers. This type of conductor consists of several strands of thinly insulated rectangular copper wire, the strands being laid together and covered with paper as shown in *Fig. 11*.

The individual strands are transposed at suitable places in the winding. This transposition is necessary, but is held to a minimum. High current density resulting from lower eddy-current loss and higher heat transfer between strands reduces the dimensions of the windings and the surrounding core.

Other than the windings, wherever the leakage flux enters conductive or magnetic material in the structure, eddy-current and hysteresis losses appear as stray load losses. *Fig. 12* is a field plot of the structure of the transformer. The leakage flux enters mainly at the core clamps and the tank wall.

Practical methods being employed to reduce stray load losses are illustrated in the following.

(1) Reduction of the quantity of the structure materials.

(2) Reduction of the flux density by using materials of lower permeability. Clamping structures such as the press-rings, upper and lower frames,

connecting bolts, and the end plates are reasonably reduced in materials, (normally mild steel), keeping the mechanical strength to a reliable value. Some parts of the structure where mild steel would give too much loss are effectively replaced by non-magnetic steel or non-metal.

(3) Eddy-current reduction by using materials of higher resistivity or strip metals.

In fabricating the electrostatic shield rings, a very thin foil of a high-resistance alloy is wound on a bakelite ring in overlapping strips. For multiple electrostatic shield construction, each sheet consists of strips insulated from each other along their length, joined together by a common strip at one point only.

Since the shield is arranged near the windings, it is necessary to take precautions to prevent excessive eddy-current and severe over-heating.

(4) Magnetic shielding using a parallel magnetic path of lower loss or using a highly-conductive plate.

As the tank is the bulkiest part of the structure, its loss reduction is the most important. To form a parallel magnetic path, silicon steel sheets are bonded together and bolted to the tankside, greatly reducing the flux density in the tank wall as well as its losses. Alternatively a highly conductive aluminum plate diverts the stray losses in the tank into its own eddy-current losses causing compensating currents to flow in the plate and set up a flux that opposes the existing leakage flux. A series of load loss tests were carried out to assess the effect of magnetic shielding, the results being shown in *Table 1*.

Table 1 **Test Results of Load Losses**

Test Condition	Without Shield (in tank)	Without Tank	Aluminum Shield (in tank)	Magnetic Shield (in tank)
Load Loss	100	(93.5)	98.5	92.5

It is concluded that, if the shielded tank-losses are reduced to zero, the losses in the aluminum plate are slightly lower than the unshielded tank-losses; on the other hand the losses in silicon steel sheets can usually be negligibly small. Therefore we prefer to adopt the mild steel tank fitted with silicon steel sheets for large power transformers.

V. ELECTROMAGNETIC FORCES AND PRE-COMPRESS TREATMENT

The short-circuit electromagnetic forces also increase with transformer ratings. First the magnitude of radial forces is estimated by

$$F_r \propto \%Z \cdot \frac{(NI)\cdot\phi_m}{\left(\frac{wh_1}{3}+\alpha+\frac{wh_2}{3}\right)} \propto \frac{i\cdot(\mathrm{kva})^{0.75}}{\%Z}$$

and secondly the stresses produced in the windings

$$\sigma_r \propto \frac{F_r}{NQ} \propto \frac{i\cdot\phi_m}{\%Z\cdot\left(\frac{wh_1}{3}+\alpha+\frac{wh_2}{3}\right)} \propto \frac{i\cdot(\mathrm{kva})^{0.25}}{\%Z}$$

where

(NI) = ampere-turns of the winding for rated output

i = current density for rated output

and the underlying assumption is that the dimension of the active part of the transformers is in proportion to $(\mathrm{kva})^{0.25}$. Concerning concentric windings, it is easy for the windings to withstand these radial forces.

Axial forces are produced by axial asymmetries of the ampere-turns due to tappings or other winding displacement. Recently axial forces are calculated to fair accuracy with a digital computer. Adoption of logical winding arrangements, such as the parallel-wound cylindrical tap winding, reduces the axial forces. However, axial displacement caused by inaccuracy during winding assembly is inevitable.

If axial displacement is assumed as ΔH, axial force F_a is given by

$$F_a \propto \frac{\Delta H}{H}\cdot\frac{(\mathrm{kva})^{0.75}}{\%Z}$$

Thus it is essential that the windings be lined up with precaution to keep the axial displacement ΔH to a minimum.

Other than the magnitude of the forces, the pre-compress treatment has proved to have much influence on dynamic behavior of the windings. Some suggestions therefore will be given in the following, concerning the pre-compress force and the mechanical strength of the windings. A simple arrangement of two windings and its axial force distribution is assumed as in *Fig. 13*, where only displacement force P_u, and compression force P_r are taken into account.

The winding is composed of individual elements (an element may be one turn or a group of turns) and an electromagnetic driving force will be impressed on each element and the insulation between them will make an elastic structure. On this assumption, the winding may be considered as a simple elastic strut, and the same with the upper and lower insulation gaps. The equivalent length of these struts

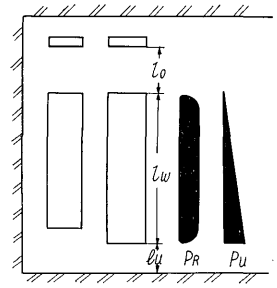

Fig. 13 Distribution of axial forces

are assumed to be l_w, l_o, l_u and the equivalent cross-sectional area, S_w, S_o, S_u respectively.

If the complex oscillatory nature of the forces is neglected, the shrinkage of the winding Δl_w and of the insulation gap Δl_u would be given by

$$\Delta l_w \propto (0.5P_u + 0.85P_r)\left(\frac{l_w}{S_w}\right)$$

$$\Delta l_u \propto P_u \cdot \left(\frac{l_u}{S_u}\right)$$

When the pre-compress force P_v is impressed by coil clamps, the total shrinkage Δl of the struts will be

$$\Delta l \propto P_v \cdot \left(\frac{l_o}{S_o} + \frac{l_w}{S_w} + \frac{l_u}{S_u}\right)$$

As the pre-compress force P_v should be sufficient to prevent any gaps opening in the winding, Δl should be not less than $\Delta l_w + \Delta l_u$, so the P_v is given by

$$P_v \propto \frac{(0.5P_v + 0.85P_r) \cdot \left(\frac{l_w}{S_w}\right) + P_u\left(\frac{l_u}{S_u}\right)}{\frac{l_o}{S_o} + \frac{l_w}{S_w} + \frac{l_u}{S_u}}$$

Although the presence of gaps through the short-circuit does not necessarily mean damage, the windings should be fully stabilized during assembly and remain so in long years of service.

In practice pre-compress force is determined not only by short-circuit forces but also by empirical factors like shrinkage of pressboads during drying treatment and aging.

VI. NOISE REDUCTION

To solve the community noise problem caused by the recent need for installing large transformer stations in city areas, we have developed the " concrete enclosure system."

The most marked feature of this system is that the transformer is completely enclosed with concrete barrier walls and the bushings are drawn out at its pocket through openings in the roof. Another beneficial result of the adoption of this system is a reduction of height to half that of conventional concrete building systems using " wall-through bushing "

This has proved to produce a noise level reduction of more than 30 dB compared with transformers built in accordance with current practice.

VII. TRANSPORT

Transformers have to be transported completely assembled with their oil tank in order to protect the very carefully manufactured windings. Transportation in parts is out of the question unless unfavorable transport conditions exist.

Fuji Electric introduced the cantilever type wagon for railway transport in Japan. This cantilever type wagon, called " Schnabel-Shiki 240 ", has a maximum weight capacity of 240 tons and has 24 axles. The transformer, in its self-supporting tank, is suspended between two cantilevers which are each carried on their own bogie trucks. A special suitable form of tank called " Fahrbar type " has been developed.

Fig. 14 Transportation of 275 kv 345 Mva transformer

The reduction in the permissible loading width caused by curves in the railway would be considerable, because of the larger transit of the center of gravity of the heavier piece, and the enlarged wagon length, which the larger number of axles requires due to the maximum permissible axle load of 14 tons on the railway.

To solve these difficulties, the 240 tons cantilever wagon is provided with the weight bearing and the pivot bearing separately. The center of the pivot bearing is positioned closer to the transformer and the weight bearing supports the weight of the cantilever and transformer with two roller bearing wheels, which permits lateral displacement of the transformer outward at curves, and thus the loading width available is increased.

Fig. 14 shows the transportation of a 3ϕ 275 kv 345 Mva transformer.

Marine transportation places no practical limitations on transformer output. It is of course important to ensure that adequate unloading facilities and a vehicle for further transport to the site will be available.

In our works, we can assemble and carry even the bulkiest unit by means of two heavy cranes with a maximum capacity of 600 tons. Fuji Electric has (adjacent to its transformer works, in Chiba Pref.) a shipping port which, together with post-crane installations, can receive ships of the 10,000 ton class. These circumstances are quite advantageous for overseas transportation.

VIII. TERTIARY CURRENT LIMITING REACTOR

Large power transformers for substations are generally three winding transformers, the tertiary winding of which is usually 1/3 of the main two windings in kva.

As the impedance between m.v. and l.v. windings is usually smaller, sufficient consideration must be given to the short-circuit strength of the tertiary

winding itself, or the system connected. The impedance between the l.v. winding and the m.v. or h.v. windings should be increased to restrict the short-circuit capacity of the tertiary system connected.

Methods to achieve this are,

(1) Increase the width of the l.v. winding as well as its insulation distance to the adjacent winding.
(2) Connect an impedance, such as a reactor, to the l.v. winding.

The former necessitates larger sizes and weight, because increasing the impedance between the m.v. and l.v. windings by increasing the distance between the windings also increases the height and diameter of the windings and the overall dimensions of the transformer.

The latter method is to connect a current limiting reactor in series with the l.v. winding.

This reactor winding is similar to the transformer winding without the core, and is enclosed with magnetic sheet shielding to reduce the stray load losses due to the reactor flux. This magnetic shielding is four limbed or combined sets of two limbed paths, according to the dimmensional requirements, and is arranged in a corner of the transformer tank. The current limiting reactor is connected in delta, or in open star, to the line and thus is adapted to the zero-sequence impedance of the h.v. and l.v. windings.

The increase in dimensions or materials by use of reactors is smaller than the method described above. Conseqnently the tertiary current limiting reactor is an effective measure in keeping pace with the demand for greater output per transformer with- out exceeding the railway loading gauges.

IX. CORONA DETECTION

Through laboratory research and measurement the study of inner corona within transformers has been continued in recent years. Corona test is a promising non-destructive test, and the absence of corona indicates that a transformer is well constructed and has extra design and manufacturing margins for a long, reliable service life.

The detection of corona within a transformer winding is rather difficult because it can be measured not at its place of occurrence after the transformer is completely assembled, but at a terminal to which its effect may be transmitted in a more or less attenuated state. Further the problem of locating corona as well as eliminating external interference remains. Of the NEMA method, the corona pulse method, and the acoustic method; the corona pulse method is recommended as a test for transformers because it is simple, accurate, and indicates the corona intensity with regard to its destroying effects. In power frequency tests the induced test, shown in *Fig. 15,* is the popular method of testing extra-high voltage windings, and has been adapted successfully

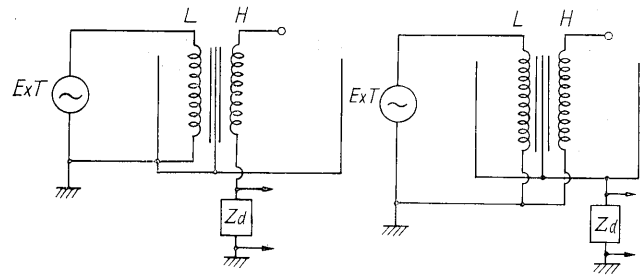

(a) Tank-earthed (b) Tank not earthed

Fig. 15 Examples of corona test circuit (Induced test)

to locate corona occurrence.

As for detectors, the shunt circuit of self inductance and capacitance (L_d, C_d) is the most advantageous because of its high sensitivity. A new corona locating method has been developed for windings of higher series capacitance, such as the oscillation-free cylindrical winding, in which a simpler corona pulse equivalent circuit can be assumed and hence is easier to analyze.

If a sample charge Q_a is given to the line terminal, the voltage V_d transmitted to the detector is given by

$$V_d=(A\cos\omega_A t+B\cos\omega_B t)Q_a$$

V_d has two oscillatory components of different angular frequency. Coefficient A, B, and angular frequency, ω_A, ω_B are determined from transformer circuit constants and the L_d and C_d of the detector. By adjusting L_d, and C_d, the ratio of angular frequency ω_A to ω_B is selected to be approximately 1.5. If angular frequency ω_A and ω_B is thus fixed, ω_A and ω_B are independent of corona occurence within the winding. On the other hand the amplitude of A and B depends of the place of corona occurence. Accordingly, location of corona occurence is possible by analyzing the transmitted waveform. This technique has been adopted in the corona measurements of oscillation-free cylindrical layer windings of large power transformers. It has proved that these transformers have a margin such that no corona is detected at 1.3 times the working voltage.

The detection of impulse corona is much more complex and difficult because of the heavier impulse charging current in the test piece, pulse waveform similarity to the impressed impulse voltage, and the disturbance induced in the measuring system. These difficulties have been overcome, and we have succeeded in detection of impulse corona for some insulations.

Fig. 16 shows an example of corona current in an oil gap. Some of the observed features are:

(1) Impulse corona in oil shows a considerable time lag in the discharging process.
(2) The duration of impulse corona is aboat 0.1 μs, and its interval of occurrence is $10^{-7}\sim10^{-6}$ sec.

When the inner N-connection of the oscillation-

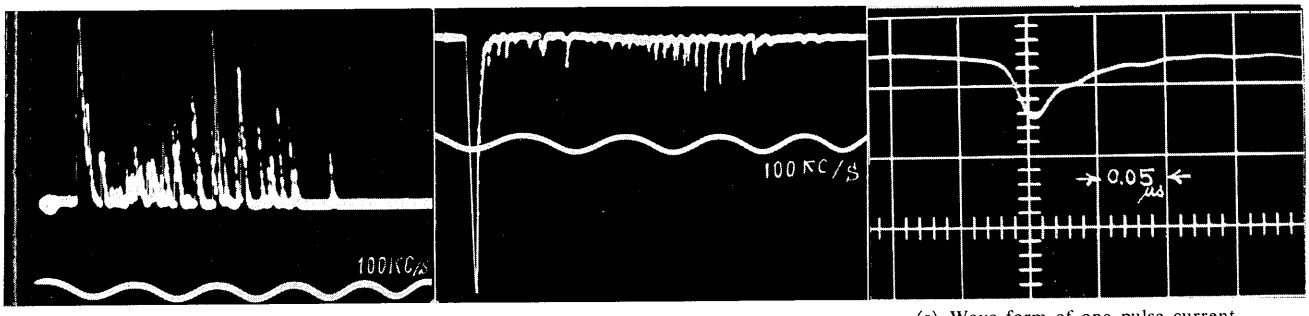

(a) (+) 100 kv impulse wave (b) (−) 100 kv impulse wave (c) Wave form of one pulse current [(−) 100 kv impulse wave]

Fig. 16 Wave forms of corona current in oil gap

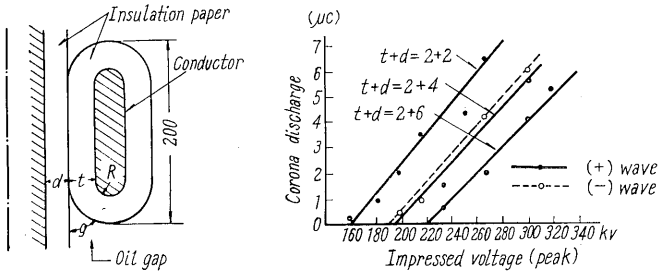

Fig. 17 Impulse corona test on a test piece

free cylindrical layer winding was investigated, impulse corona test was carried out on many test pieces of the connection lead. Test results are shown in *Fig. 17* and indicate that:

(1) Corona charge increases approximately in proportion to the impressed voltage.

(2) Impulse corona starting voltage is obtained from *Fig. 17,* by extrapolating the line to zero.

(3) Destruction voltage is 1.6 times higher than impulse corona starting voltage.

X. COOLING

Large power transformers are nearly always equipped with some sort of auxiliary cooling. The forced-oil fan-cooling system that uses unit coolers is particularly popular in our country. Some problems concerning the cooling of large power transformers are discussed in the following.

(1) Directed flow system

In transformers which employ the forced-oil system, it is ineffective to circulate the oil merely from the coolers into the tank. It should be arranged that the oil may uniformly reach every active part of the transformer. The oil flowing out of the coolers is collected through the walls of the tank once into the lower frame and is branched off directly by oil guides into the windings and the core. The branch flows of oil are managed to match not only the heat loss of each portion but also the head loss of each oil path.

In oscillation-free cylindrical layer windings, the flowing oil is made to take a direct course in vertical ducts. In disc windings the flowing oil is caused to pass througe the vertical ducts as well as the horizontal ducts by a zig-zag course with a suitable arrangement of ducts.

(2) Prevention of local overheating

It is essential to take precautions to prevent transformers from local overheating which is caused by the leakage flux and reduced insulation space resulting from the demensional restrictions. The local winding loss can be calculated with fair accuracy and the temperature rise of each part of the winding predicted. Uniform insulation, which is enabled by non-oscillatory winding, dispensing with the strengthened end insulation; and common-insulated conductor, in which the temperature gradient between strands is much reduced, are effective in surpressing overheating. The temperature rise in structures, which has some complex aspects, is ascertained, if necessary, by attaching thermocouples and conducting a heat run test. Magnetic tank-shielding has been found useful to prevent the tank from overheating.

(3) U-fin radiator

For the forced-oil fan-cooling system, Fuji Electric adopts U-fin radiators for oil-to-air heat exchange. Through the U-fins attached on the surface of cooling pipes, the cooling wind effectively agitates the stagnant air film; with lower machinery loss. Furthermore a spiral is inserted in the cooling pipe to promote turbulent flow of oil and to improve oil-to-pipe heat exchange.

(4) Separate type forced-oil self-cooling system

In the concrete enclosure system (in which super-low noise level is achieved) the forced-oil self-cooling system with separate radiators has been adopted thereby completely dispensing with cooling fans. The radiators are installed in the iron structure apart from the transformer; the piping system connecting them. The oil feed pumps are inserted respectively to each pipe in order to restrict the head loss of the oil passage as well as to reduce auxiliary machinery loss.

Vibration-proof flexible joints are inserted in the oil feed line at the enclosure wall to prevent

the acoustic energy from propagating to the radiators.

XI. ON-LOAD TAP-CHANGER

The recent trend on-load tap-changing equipment is illustrated as follows:

(1) The on-load tap-changing equipment is put into the tank to achieve the totally enclosed type reliability and is transported in a completely assembled state.

(2) As the reactor type requires a large space, the resistor type has become popular for its compactness and other excellent features and this system will be used on all future products. Since the introduction of the on-load tap-changer, Fuji Electric has always adopted the resistor switch, the so-called "Jansen switch" and therefore has acquired abundant experience in its application to a large number of transformers. The basic distinctive features of the resistor type are listed below.
   (a) Quick motion spring and 4-leg link mechanism.
   (b) Non-stop operation at intermediate position.
   (c) Cross current between taps is restricted by resistor.
   (d) Power factor of arc current during break-off $=1$.
   (e) Good arc surpression, arc time being within 1/2 cycle.
   (f) Carbonizing of oil and consumption of contacts are both negligible.

(3) To cope with the increase in current ratings, the arcing contacts are divided into parallel pieces and balancers are inserted between these parallel circuits. Thus the flow of current is balanced causing effective decrease in the erosion of the contacts. The life and durability of the equipment has been increased and the replacement of contacts is not necessary for a long period of service life.

(4) The hot-line oil filtering system has been used generally. An oil filtering device filters or changes the oil of the diverter switch chamber without stopping operation of the transformer.

XII. COMPUTER USE

The digital computer is now being used successfully for preliminary and complete transformer design and for various transformer development applications. Some of these are referred to in other chapters.

With only performance data as input, the computer automatically designs a transformer covering 3ϕ 1~ 500 Mva to meet requirements of the specifications.

Moreover the computer carries out very rapidly a large number of designs and thus assists the designer in his pursuit of an optimum design. *Fig. 18* shows an example of the output data of a 3ϕ 60 cps 300/300/90 Mva 275/154/22 kv on-load tap-changing transformer. Although programing and debugging effort is tedious, this computerized design program frees our engineering staff to do creative engineering instead of purely routine mathematical work.

XIII. CONCLUSIONS

In this paper the general aspects of Fuji Electric's recently developed techniques for large power transformers have been discussed. Through such developments as described here, together with the results of present investigations, we shall be able to satisfactorily meet demands for still greater transformer ratings.

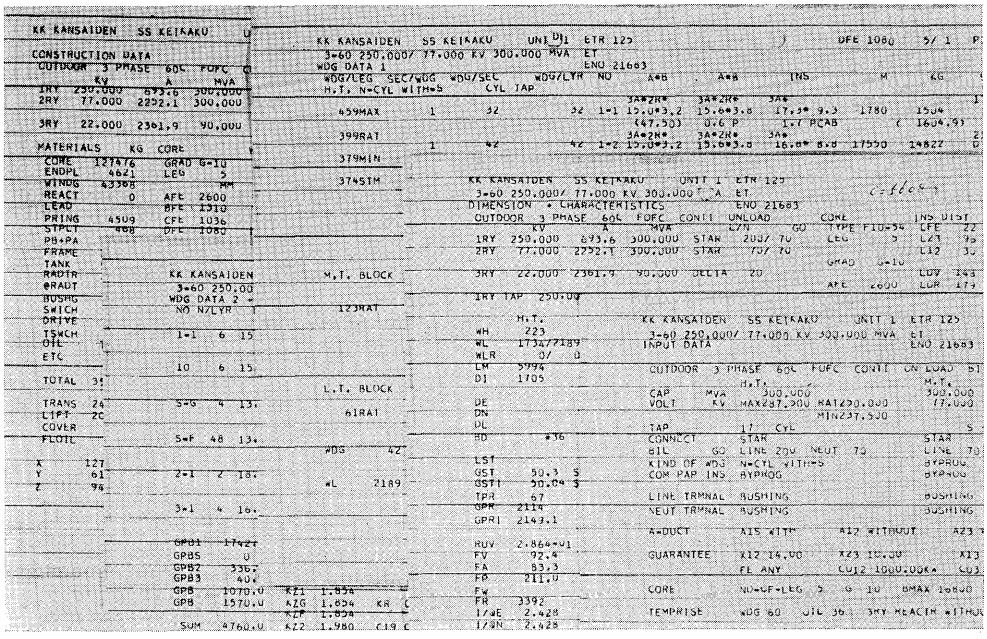

Fig. 18 An example of output data of transformer design